Research Article J. Electrochem. Sci. Technol., 2022, 13(2), 208-212

# Effect of Temperature on the Deterioration of Graphite-Based Negative Electrodes during the Prolonged Cycling of Li-ion Batteries

Jin Hyeok Yang[1], Seong Ju Hwang[2], Seung Kyu Chun[2], and Ki Jae Kim[1]*

[1]*Department of Energy Engineering, Konkuk University, 120 Neungdong-ro, Gwangjin-gu, Seoul 05029, Korea*
[2]*Graduate School of Energy & Environment, Seoul National University of Science & Technology, 232 Gongneung-ro, Nowon-gu, Seoul 01811, South Korea*

**ABSTRACT**

In this paper, we report the effects of temperature on the deterioration of graphite-based negative electrodes during the long-term cycling of lithium-ion batteries (LIBs). After cycling 75 Ah pouch-type LIB full cells at temperatures of 45°C (45-Cell) and 25°C (25-Cell) until their end of life, we expected to observe changes in the negative electrode according to the temperature. The thickness of the negative electrode of the cell was greater after cycling; that of the electrode of 45-Cell (144 μm) was greater than that of the electrode of 25-Cell (109 μm). Cross-sectional scanning electron microscopy analysis confirmed that by-products caused this increase in the thickness of the negative electrode. The by-products that formed on the surface of the negative electrode during cycling increased the surface resistance and decreased the electrical conductivity. Voltage profiles showed that the negative electrode of 25-Cell exhibited an 84.7% retention of the initial capacity, whereas that of 45-Cell showed only a 70.3% retention. The results of this study are expected to be relevant to future analyses of the deterioration characteristics of the negative electrode and battery deterioration mechanisms, and are also expected to provide basic data for advanced battery design.

**Keywords :** Negative Electrode, Deterioration, LIBs, Temperature Effect, EOL

*Received : 13 September 2021, Accepted : 19 October 2021*

## 1. Introduction

With recent rapid technological developments, the use of fossil fuels has drastically increased, posing environmental concerns such as global warming and air quality deterioration due to the presence of particulate matter such as fine dust. Renewable energies, such as solar energy and wind energy, have been considered as promising alternatives to reduce the use of fossil fuels [1-6]. However, the energy generated by renewable energy sources varies significantly and is dispersed because of its strong dependence on environmental conditions. Therefore, energy storage systems (ESSs) should be installed for the stable use of renewable energy systems and stable delivery in response to consumer demand [5-10].

*E-mail address: kijaekim@konkuk.ac.kr

DOI: https://doi.org/10.33961/jecst.2021.00899



Among the many batteries used in ESSs, lithium-ion batteries (LIBs) have been used widely as a power source because of their relatively high voltage (~4.7 V vs Li) and high energy density (650 W h $kg^{-1}$) [11]. Long-term reliability is necessary to utilize LIBs in ESSs; however, many drawbacks associated with the long-term use of LIBs have been reported recently in ESSs employing LIBs. In many cases, these drawbacks are related the locations where the ESSs are installed (e.g., in a hot and humid climate). The electrochemical performance, such as the cycle-life performance, of LIBs installed in ESSs thus deteriorates quickly in comparison to the performance of LIBs operated under normal conditions. Therefore, investigation of the failure mechanism or degradation behavior of LIBs with temperature is crucial for the enhanced design and effective use of LIBs in ESSs. Although there are some reports related to this degradation behavior [12-15], further studies need to be conducted, because the origin of the performance degradation of LIBs remains to be fully elucidated

due to their complex failure mechanisms.

In this study, we focused on elucidating the degradation behavior of graphite-based negative electrodes in LIBs with temperature. For this purpose, pouch-type LIBs with a capacity of 75 Ah were subjected to cycling tests at temperatures of 25°C and 45°C until their end of life (EOL) was reached. LIBs that reached their EOL were disassembled, and the physicochemical and electrochemical changes in the negative electrode before and after cycling were analyzed systematically. Thus, by analyzing the deterioration characteristics of the negative electrode with temperature, we acquired data that will be useful for the enhanced design and effective use of LIBs in ESSs in the future.

## 2. Experimental

Pouch-type LIBs with a capacity of 75 Ah composed of NCM333 as the positive electrode and graphite as the negative electrode were purchased. To analyze the degradation behavior of the negative electrode with temperature, the LIBs were subjected to cycling tests at 25°C and 45°C until they reached their EOL state, which was defined as the state at which the LIBs possessed a capacity equivalent to 70% of the initial capacity. The cut-off voltages for the charge-discharge tests were 3.0 and 1.4 V, respectively, at a rate of 1 C.

To analyze the negative electrode, LIBs that had reached their EOL were disassembled when in the fully discharged state. The negative electrode was washed twice with dimethyl carbonate (DMC) and dried at 90°C to remove the $LiPF_6$ salt. The thickness of the negative electrode was then measured using a micrometer. To measure the electrical conductivity of the negative electrode, a sample with dimensions of 1 cm × 1 cm was cut, and its resistance was measured using the four-probe method. The morphology and microstructure of the negative electrode were characterized by field-emission scanning electron microscopy (FE-SEM, Jeol JSM7000F) and energy-dispersive X-ray spectroscopy (EDX), respectively. X-ray diffraction (XRD, PANalytical Empyrean XRD system) and Raman analysis (Bruker Senterra Grating 400) with a He-Ne laser (wavelength of 943 nm) were performed to analyze the structural changes in the negative electrode.

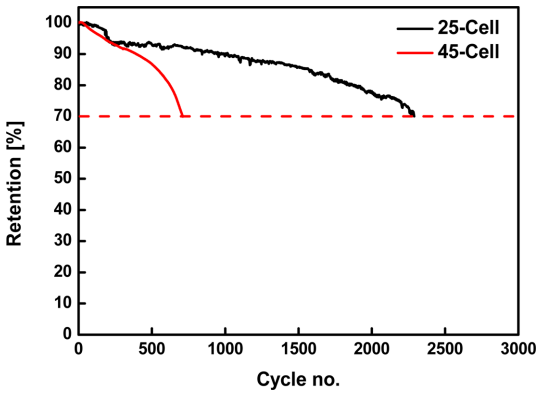


**Fig. 1.** Charge/discharge cycles reaching EOL for 25-Cell and 45-Cell.

## 3. Results and Discussion

As shown in Fig. 1, both samples undergo similar capacity changes through the initial 300 cycles, but there is a distinct difference thereafter. The LIBs that underwent cycling at 25°C (denoted as 25-Cell) showed a relatively gradual decrease in capacity and a long cycle life. On the other hand, the LIBs that underwent cycling at 45°C (denoted as 45-Cell) exhibited a rapid decrease in capacity after 300 cycles, and EOL was reached rapidly, indicating that the cycle life of LIBs is strongly affected by the temperature.

Fig. 2 shows photographs of the negative electrodes extracted from the fresh cell, 25-Cell, and 45-Cell. The surface of the negative electrode from the fresh cell was clean and moistened with the electrolyte, and showed no physical deformation (Fig. 2a). In contrast, the surfaces of the negative electrodes extracted from 25-Cell and 45-Cell exhibited many by-products caused by side reactions with the electrolyte (Fig. 2b and 2c, respectively). In particular, numerous by-products covered the surface of the negative electrode of 45-Cell. To determine the thickness of the by-products, the thickness of the negative electrode (post cycling) was measured using a micrometer. The average thickness of the negative electrodes extracted from 25-Cell was 109 μm, whereas that of the negative electrodes extracted from 45-Cell was 144 μm. Fig. 3 shows cross-sectional SEM images of the negative electrodes from 25-Cell and 45-Cell, which confirm that the by-products cause an increase in their thickness. Considering

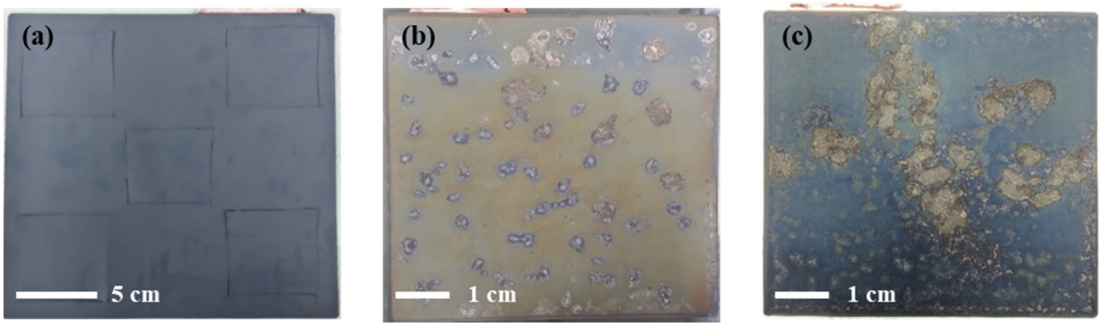


**Fig. 2.** Surface changes in the (a) fresh cell, (b) 25-Cell, and (c) 45-Cell.

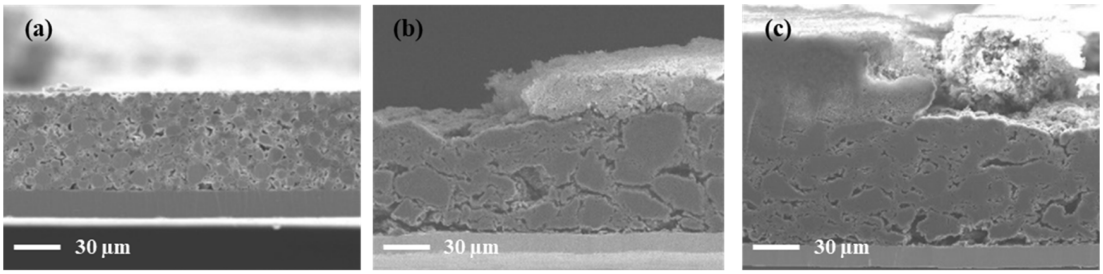


**Fig. 3.** Cross-sectional SEM images of negative electrodes in (a) fresh cell, (b) 25-Cell, and (c) 45-Cell.

the original thickness of the negative electrodes, the by-products formed on the negative electrode of 45-Cell were much thicker than those formed on the negative electrode of 25-Cell. These observations indicate that by-products form more rapidly at high temperatures.

Because the by-products that formed on the surface of the negative electrode during cycling might influence the electrical conductivity of the negative electrode, we analyzed the electrical conductivity by measuring the surface resistance of each sample. As summarized in Table 1, the average conductivity of the negative electrode extracted from the fresh cell was $3.29 \times 10^{-1}$ S cm$^{-1}$, that of the negative electrode of 25-Cell was $4.12 \times 10^{-2}$ S cm$^{-1}$, and that of the negative electrode of 45-Cell was $5.39 \times 10^{-6}$ S cm$^{-1}$. Therefore, the surface resistance was enhanced by the by-products that accumulated on the surface, and concurrently, the electrical conductivity decreased. Comparison between the results for the sample thickness and electrical conductivity confirmed the correlation between the physical and electrochemical changes.

To determine the constituents of the by-products formed on the surface of the negative electrode, FE-SEM and EDX were performed. As shown in Fig. 4, carbon (C) has a higher weight and atomic composition than oxygen (O) on the surface of the negative electrode extracted from the fresh cell. Furthermore, phosphorus (P), fluorine (F), C, and O are equally detected in the by-products of both samples. This indicates that these by-products were formed by continuous electrolyte decomposition on the surface of the negative electrode during repeated cycling. In addition, we can speculate that the temperature did

**Table 1.** Changes in electrical conductivity of negative electrodes.

| Sample | Fresh cell [S/cm] | 25-Cell [S/cm] | 45-Cell [S/cm] |
|---|---|---|---|
| 1 | $2.88 \times 10^{-1}$ | $3.12 \times 10^{-2}$ | $3.70 \times 10^{-6}$ |
| 2 | $3.62 \times 10^{-1}$ | $4.53 \times 10^{-2}$ | $8.90 \times 10^{-6}$ |
| 3 | $3.90 \times 10^{-1}$ | $4.20 \times 10^{-2}$ | $3.42 \times 10^{-6}$ |
| 4 | $3.13 \times 10^{-1}$ | $3.41 \times 10^{-2}$ | $8.80 \times 10^{-6}$ |
| 5 | $2.92 \times 10^{-1}$ | $5.33 \times 10^{-2}$ | $2.11 \times 10^{-6}$ |
| Avg. | $3.29 \times 10^{-1}$ | $4.12 \times 10^{-2}$ | $5.39 \times 10^{-6}$ |

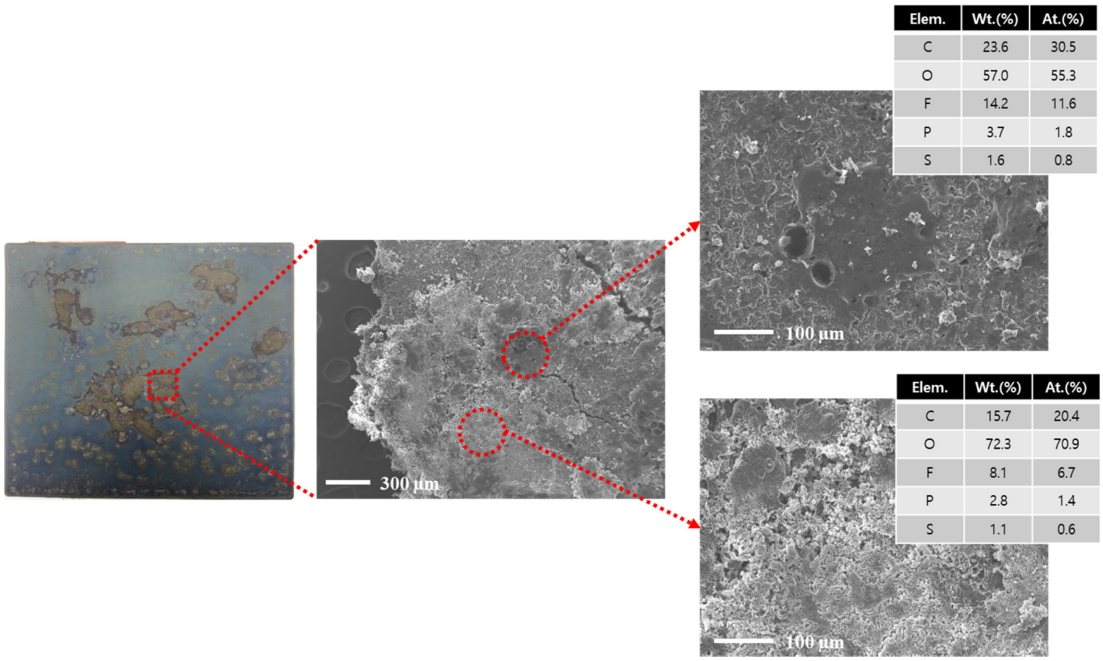


**Fig. 4.** Analysis of the by-products on the surface of negative electrodes.

not affect the constituents of the by-products, but instead influenced the amount of the by-products.

In terms of the physical degradation of the negative electrodes, thus far, we have determined that by-product accumulation on the surface of the negative electrodes was independent of the operating temperature during cycling, but the amount of the by-products was dependent on the operating temperature. Additionally, we found that the electrical conductivity of the negative electrode was strongly affected by the formation of by-products. XRD and Raman analyses were performed to further investigate the degradation behavior of the negative electrode samples. The XRD (Fig. S1) and Raman (Fig. S2) results indicated no significant differences in any of the negative electrodes, before or after cycling, suggesting that structural changes could not be confirmed.

Fig. 5 shows the voltage profiles of the fresh and negative electrodes cycled at a rate of 1C in a half-cell configuration using Li metal as the counter electrode. The negative electrode of 25-Cell exhibited an 84.7% retention of the initial capacity, but that of 45-Cell showed only a 70.3% retention of the initial capacity. In addition, the polarization (indicated by a voltage drop) of the negative electrode extracted from the fresh cell was much lower than those of the cycled negative electrodes extracted from 25-Cell and 45-Cell. This is mainly attributable to the increased resistance of the cycled negative electrodes resulting from the formation of by-products. Interestingly, the polarization of the negative electrode of 25-Cell was much lower than that of 45-Cell. This result occurred because large amounts of thick

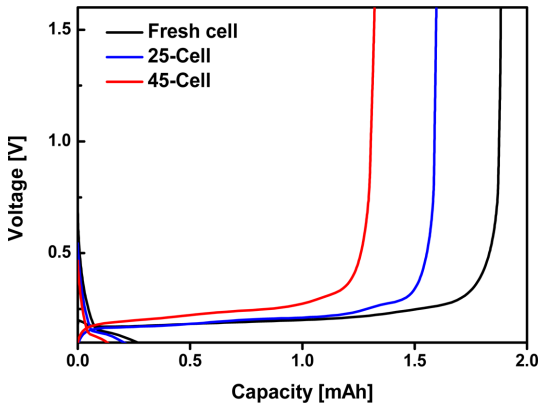


**Fig. 5.** Voltage profiles of the fresh cell, 25-Cell, and 45-Cell at a rate of 1C.

by-products covered the surface of the negative electrode of 45-Cell, leading to a larger increase in the electrical resistance.

Based on the physical and electrochemical analyses of the cycled negative electrodes, their performance degradation mechanism was considered. Regardless of the operating temperature during cycling, we found that the by-products produced by electrolyte decomposition were widely distributed on the surface of the negative electrode after EOL had been reached. In addition, the amount and thickness of the by-products were affected greatly by the operating temperature during cycling, such that much more and thicker by-products formed on the surface of the deteriorated negative electrode at a high temperature. Electrical conductivity measurements revealed that the cycled negative electrodes exhibited a significantly increased resistance because of the by-products covering their surface. The capacity fading of the cycled negative electrodes may thus be attributed to the increased interfacial resistance due to the formation of by-products.

## 4. Conclusions

The degradation behavior of graphite-based negative electrodes in LIBs with temperature was analyzed to provide a basis for the enhanced design and more effective use of LIBs in ESSs in the future. The negative electrodes used in 45-Cell had more by-products and a lower electrical conductivity than those used in 25-Cell. Moreover, the cycle life of 45-Cell deteriorated approximately 31% faster than that of 25-Cell. In terms of electrochemical properties, 45-Cell showed only a 70.3% retention of the initial capacity in comparison to the 84.7% retention of the initial capacity exhibited by 25-Cell. This study confirmed that temperature affects the deterioration of graphite-based negative electrodes. We expect that these results will be relevant to understanding the deterioration characteristics of negative electrodes in future studies on battery deterioration mechanisms.

## Acknowledgement

Jin Hyeok Yang and Seong Ju Hwang contributed equally to this work. This work was supported by the Technology Innovation Program (20011379) funded by the Ministry of Trade, Industry & Energy (MOTIE, Korea).

## Supporting Information

Supporting Information is available at https://doi.org/10.33961/jecst.2021.00899

## References

[1] K. Li, J. Yan, H. Chen, Q. Wang, *Appl, Therm. Eng.,* **2018**, *132*, 575-585.
[2] M. M. Thackeray, C. Wolverton, E. D. Isaacs, *Energy Environ. Sci*., **2012**, *5(7)*, 7854-7863.
[3] Z. Li, A. Khajepour, J. Song, *Energy*, **2019**, *182*, 824-839.
[4] Y. Hamakawa, Background and Motivation for Thin-Film Solar-Cell Development, *Thin-Film Solar Cells*, Springer, **2004**, 1-14.
[5] S. Hwang, M. Batmunkh, M. J. Nine, H. Chung, H. Jeong, *Chem. Phys. Chem.,* **2015**, *16(1)*, 53-65.
[6] S. Batel, *Energy Res. Soc. Sci.,* **2020**, *68*, 101544.
[7] K. J. Kim, M. S. Park, Y. J. Kim, J. H. Kim, S. X. Dou, M. Skyllas-Kazacos, *J. Mater Chem. A*, **2015**, *3(33)*, 16913-16933.
[8] K. J. Kim, Y. J. Kim, J. H. Kim, M. S. Park, *Mater. Chem. Phys.,* **2011**, *131(1-2)*, 547-553.
[9] K. J. Kim, M. S. Park, J. H. Kim, U. Hwang, N. J. Lee, G. J. Jeong, Y. J. Kim, *Chem. Commun.,* **2012**, *48(44)*, 5455-5457.
[10] Y. Yang, S. Bremner, C. Menictas, M. Kay, *Renew. Sustain Energy Rev.*, **2018**, *91*, 109-125.
[11] G. Liang, V. K. Peterson, K. W. See, Z. Guo, W. K. Pang, *J. Mater. Chem. A*, **2020**, *8(31)*, 15373-15398.
[12] D. Ouyang, J. Wng, M. Chen, J. Liu, J. Wang, *Int. J. Energy Res*., **2020**, *44(1)*, 229-241.
[13] Y. Saito, M. Shikano, H. Kobayashi, *J. Power Sources*, **2013**, *244*, 294-299.
[14] S. Yang, Y. Hua,. D. Qiao, Y.Lian, Y. Pan, Y. He, *Electrochimica Acta*, **2019**, 326.
[15] D. Ouyang, J. Weng, M. Chen, J. Wang, *J Energy Storage*, **2020**, 28.